Dalton Transactions

Accepted Manuscript

ROYAL SOCIETY OF CHEMISTRY

www.rsc.org/dalton

Journal Name

ARTICLE

A Trinuclear Ruthenium Complex as Highly Efficient Molecular Catalyst for Water Oxidation

Received 00th January 20xx,
Accepted 00th January 20xx

DOI: 10.1039/x0xx00000x

www.rsc.org/

L. L. Zhang,[a] Y. Gao,*[a] Z. Liu,[a] X. Ding,[a] Z. Yu[a] and L. C. Sun*[a,b]

A trinuclear ruthenium complex **3** was designed and synthesized with the ligand 2,2'-bipyridine-6,6'-dicarboxylic acid (bda), and we found that this complex can work as highly efficient molecular catalyst for water oxidation in homogeneous systems. This trinuclear molecular water oxidation catalyst **3** displayed much higher efficiencies in terms of turnover numbers and initial oxygen evolution rate than its counterparts, a binuclear catalyst **2** and a mononuclear catalyst **1**, in both chemically driven and photochemically driven water oxidation based on either the whole catalytic molecules or the active Ru centers. The reasons for the superior performance of the catalyst **3** were discussed and we believe that the multinuclear Ru centers involved in a single molecule are indeed beneficial for enhancing the opportunity of the formation of O-O bond through intramolecular radical coupling pathway.

Introduction

Natural photosynthesis (NPS), utilizing solar energy to convert water and carbon dioxide into carbohydrates in photosynthetic organisms, produces essential energy and resources to sustain the natural creatures on earth.[1-3] Inspired by the NPS, artificial photosynthesis is consistently regarded as one of the best ways to obtain abundant sustainable and clean energy to meet the decreasing traditional energy resources and the arising environmental concerns. At present, this hot research topic has attracted great attention around the world and much effort has been paid on functional mimics of the active site of photosynthesis. The most prospective method among them is the production of hydrogen or the reduction of carbon dioxide through light driven water splitting. While in both processes, water oxidation is the key challenge which provides the important electrons and protons to ensure the solar-to-fuel conversion. Therefore, many attempts have been carried out on development of highly efficient water oxidation catalysts based on transition metal complexes, such as manganese (Mn),[4-8] Ru,[9-19] iridium (Ir)[20-23] in which Ru-based catalysts have displayed the best performance so far.

Among the developed Ru-based catalysts, a mononuclear Ru-bda (bda = 2,2'-bipyridine-6,6'-dicarboxylic acid) type of catalysts has been developed by our group and displayed significant activities on water oxidation with a bimolecular radical coupling reaction mechanism.[14] Based on this reaction mechanism, several binuclear Ru-bda catalysts have been designed and synthesized for catalytic water oxidation and considerably high turnover numbers (TONs) were obtained based on the generated oxygen.[17] The results indicated that O-O bond formation should occur in binuclear Ru-bda catalyst units through intramolecular radical coupling pathway.

In this present work, we report a trinuclear Ru-bda catalyst **3** together with a reference binuclear Ru-bda catalyst **2**, their structures are shown in Chart 1. Experimental results display that further increase of the catalyst unit in a single molecule leads to better catalytic activity, very likely due to the increased opportunities of intramolecular O-O bond formations. The enhancing performances of catalyst **3** on catalytic water oxidation were studied and discussed in this paper.

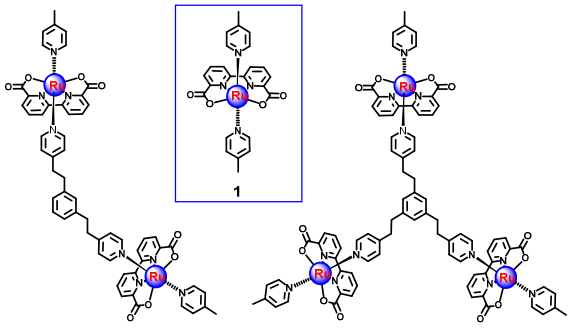

Chart 1. Structures of catalysts **1**–**3**.

Results and discussion

[a] State Key Laboratory of Fine Chemicals, DUT-KTH Joint Education and Research Center on Molecular Devices, Dalian University of Technology (DUT), Dalian 116024, China.
[b] Department of Chemistry, School of Chemical Science and Engineering, KTH Royal Institute of Technology, Stockholm 10044, Sweden.

Electronic Supplementary Information (ESI) available: [details of any supplementary information available should be included here]. See DOI: 10.1039/x0xx00000x

Synthesis and characterization of complexes 2 and 3.

Complexes **2** and **3** were synthesized by linking the Ru(bda)$(pic)_2$ unites through flexible chain containing benzene similar to the synthetic route of complex Ru(bda)$(pic)_2$ **1** (pic = picoline). Their structures were fully characterized by ^{1}HNMR spectroscopy, as well as HR-MS and elemental analysis (Figure S1-S4). The ^{1}HNMR spectrum of complex **2** displays that the proton resonances of the equatorial ligand are assigned to the doublet at δ = 8.65 and 7.88 and triplet at δ = 7.81, of the axial ligand are assigned to the triplet 7.53 and the multiplet (two doublet) at δ = 7.1. Protons on the benzene are assigned to the triplet at δ = 7.05 covered partly by the multiplet and double at δ = 6.87 and singlet at δ = 6.77. Comparing to complex **2**, the proton resonances of equatorial ligand of complex **3** are found at positions of 2' and 3' are coincident leading to the multiplet. While the proton resonances of axial ligand are assigned to the doublet at δ = 7.07 and 6.96 belong to the protons at positions of H5 and H5', respectively. The protons at position of H4' display a broad singlet because of the highly symmetrical structure. The protons affiliation indicates the correct structures of complexes **2** and **3**. The HR-MS signals at m/z = 1185.1423 and 1727.1951 are assigned to the species of $[\mathbf{2}+Na]^+$ and $[\mathbf{3}+Na]^+$ confirm again the correct structures of complexes **2** and **3** above .

Electrochemistry of complexes 1–3.

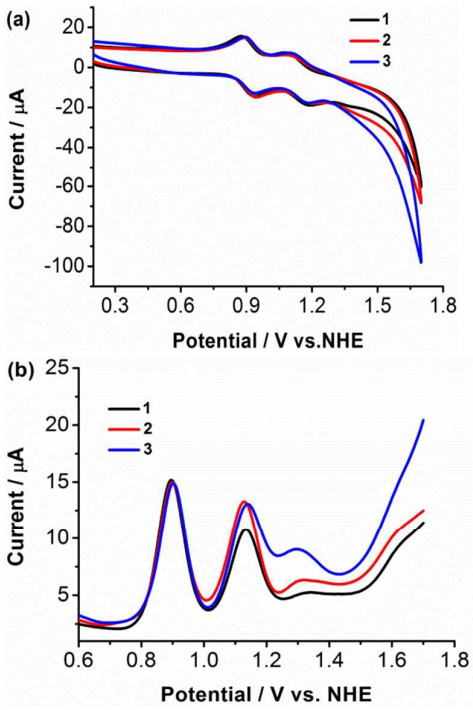

Figure 1. CVs (a) and DPVs (b) of complexes **1** (black line, 1×10^{-3} M), **2** (red line, 5×10^{-4} M) and **3** (blue line, 3.3×10^{-4} M) in CF_3SO_3H (pH 1.0) containing 20% CH_3CN with the glassy carbon as the working electrode, Pt wire as the counter electrode, Ag/AgCl as the reference electrode, scan rate 50 mV/s, $E_{NHE} = E_{Ag/AgCl} + 0.20$.

Cyclic voltammograms (CVs) and differential pulse voltammograms (DPVs) of complexes **1** (1×10^{-3} M), **2** (5×10^{-4} M) and **3** (3.3×10^{-4} M) were taken in CF_3SO_3H (pH = 1.0) aqueous solution containing 20% CH_3CN as shown in Figure 1. The CV curve of complex **2** (Figure 1a, red line) displays two reversible redox peaks at $E_{1/2}$ = 0.92 and 1.14 V (vs. NHE), which are assigned to the redox couples of Ru^{II}/Ru^{III}-OH_2 and Ru^{III}-OH_2/Ru^{IV}-OH, respectively. The complex **3** (Figure 1a, blue line) exhibits similar profiles of $Ru^{II/II}$I and $Ru^{III/IV}$ redox processes at $E_{1/2}$ = 0.92 and 1.15 V (vs. NHE), respectively. The profiles of $Ru^{II/III}$ and $Ru^{III/IV}$ redox processes of complexes **2** and **3** are quite similar to the complex **1** (Figure 1a, black line), at $E_{1/2}$ = 0.89 and 1.12 V (vs. NHE). The potential differences between the anodic (E_{pa}) and cathodic (E_{pc}) peaks of $Ru^{II/III}$ redox couples are calculated to be about 59 mV. This electrochemical behavior demonstrates the single-electron redox process of $Ru^{II/III}$ redox couple and indicates that Ru centers of the dinulcear complex **2** and the trinuclear complex **3** are independent at low oxidation stage.

In addition to the oxidation processes of Ru^{II}/Ru^{III}-OH_2 and Ru^{III}-OH_2/Ru^{IV}-OH, the oxidation peak at E_{pa} = 1.30 V (vs. NHE) is also detected, respectively, for catalysts **1**, **2** and **3** in the DPV measurements (Figure 1b), which are assigned to the oxidation process of Ru^{IV}-OH/Ru^{V}=O. Beyond this oxidation peak, the catalytic current of catalyst **3** is found obviously higher than that of catalysts **1** and **2**, which indicates that catalyst **3** possesses superior catalytic activity on water oxidation.

Water oxidation by chemical oxidants.

The water oxidation abilities by chemical oxidants of the complexes **1**, **2** and **3** were investigated in CF_3SO_3H (pH 1.0) aqueous solution using $(NH_4)_2[Ce(NO_3)_6]$. For comparison, the concentrations of 1×10^{-7} M for catalyst **1**, 5×10^{-8} M for catalyst **2** and 3.3×10^{-8} M for catalyst **3** were selected to control the same amount of catalytic Ru centers involving in catalytic water oxidation systems. The oxygen evolution was detected with an oxygen sensor and calibrated by GC, as shown in Figure 2. Based on the generated oxygen and catalyst molecules, a high turnover number (TON) of 44412 for catalyst **2** (red line) and a much higher TON of 86498 for catalyst **3** (blue line) were obtained as shown in Figure 2a. The initial turnover frequencies (TOFs) are calculated to be 68 and 126 s^{-1}, respectively. Based on the amount of catalyst molecules, the TON of catalyst **3** is almost twice as much as that of catalyst **2**. Even based on the number of Ru catalytic centers, the TON of 28832 and TOF of 42 s^{-1} per Ru center of catalyst **3** are still much higher than those of catalyst **2** (TON of 22206 and TOF of 34 s^{-1} per Ru center) and the reference reported ruthenium dimer (TON of 21420 and TOF of 20 s^{-1} per Ru center)[17], as shown in Figure 2b. Both binuclear catalyst **2** and trinuclear catalyst **3** display significantly higher efficiency than mononuclear catalyst **1** (TON of 1460 and TOF of 3.8 s^{-1}). These results illustrate the O-O bond formations is easier in catalyst **2** and **3** during the catalytic water oxidation process

and implies the mechanism changes from intermolecular reaction of catalyst **1** to intramolecular reaction of catalysts **2** and **3**.

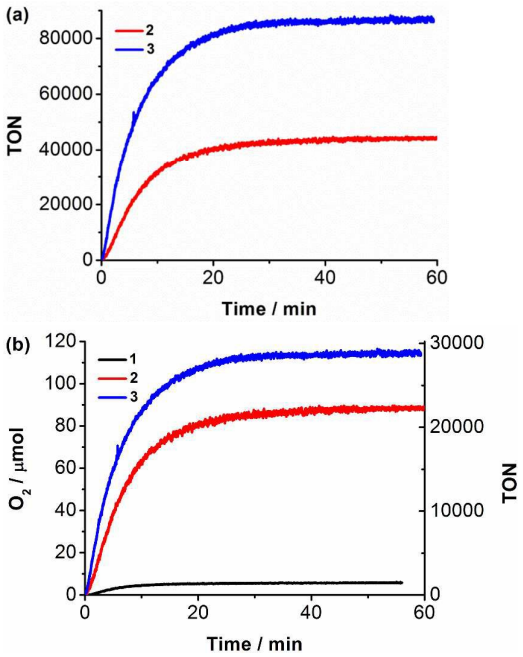

Figure 2. Oxygen evolution of catalysts **1** (1×10^{-7} M) (black line) and **2** (5×10^{-8} M) (red line) and **3** (3.3×10^{-8} M) (blue line) with $(NH_4)_2[Ce(NO_3)_6]$ (5.0×10^{-2} M) as oxidant in CF_3SO_3H (pH 1.0) solution. (a) TONs based on the number of catalyst molecules. (b) TONs based on the number of ruthenium catalytic units.

Additionally, as reported,[25] local enrichment of the catalytic centers can increase the catalytic activity of mononulcear catalyst **1**. The reported reference results showed that the catalytic activity of catalyst **1** was found increase obviously with the number of Ru centers rising from 1 to 7 in each nanocage.[25] Therefore, the better performance of catalyst **3** indicates that more Ru centers involved in a single molecular catalyst are beneficial to enhance the catalytic activities. The insight is that multinuclear units in a single molecule indeed increase the opportunity of O-O bond formation through intramolecular radical coupling.

Additional experiments on studying the performance of these catalysts have been carried out by using different amount of oxidant in the systems. Keeping the same concentrations of catalysts **2** (5×10^{-8} M) and **3** (3.3×10^{-8} M), alteration of the concentration of Ce(IV) from 2.5×10^{-2} M to 7.5×10^{-2} M leads to different TONs based on ruthenium catalytic centers, as shown in Figure 3a. It is obvious that the highest TONs of catalysts **2** and **3** were obtained with the Ce(IV) concentration of 5×10^{-2} M. Moreover, the initial TOFs of catalysts **2** and **3** based on the Ruthenium catalytic unites under different concentrations of Ce^{IV} were calculated according to the data from Figure S5 (Figure 3b). TOFs of catalysts **2** and **3** are calculated to around 30 s^{-1} and 40 s^{-1}, respectively. The result confirms that the initial oxygen evolution rate is zero order to the concentrations of Ce^{IV} under our experimental condition. All these results indicate that utilization of lower or higher concentration of Ce(IV) seems do not benefit for catalytic water oxidation. Higher concentration of Ce(IV) might accelerate the decomposition of the catalysts. Nevertheless, catalyst **3** consistently displays higher efficiency than catalyst **2** in the whole experiments. When using high concentrations of Ce(IV) (more than 5×10^{-2} M), lower decreasing tendency of TONs of catalyst **3** is found than that of catalyst **2**. The reason might be due to that when one of the metal-based active centers is damaged by excessive oxidant, catalyst **3** can still carry O-O bond formation through intramolecular radical coupling with the two remaining active centers. On the contrary, after losing one active center, catalyst **2** has to perform O-O bond formation through intermolecular radical coupling or nucleophilic attack of water upon the survived single active center, particularly in such a low catalyst concentration.

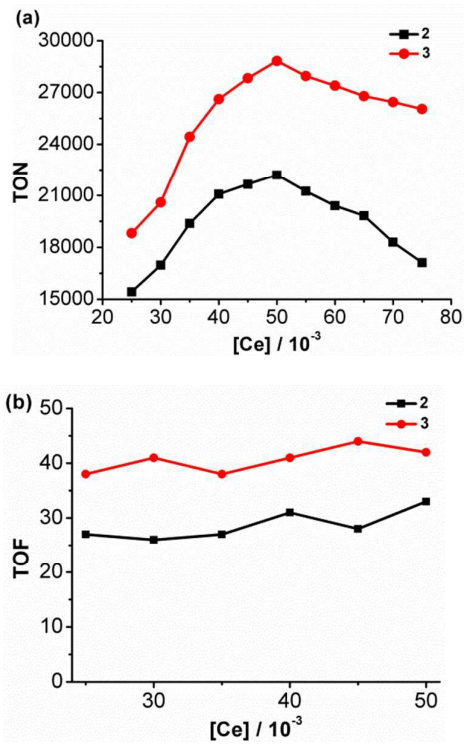

Figure 3. TONs (a) and initial TOFs (b) of catalysts **2** (5×10^{-8} M) (black line) and **3** (3.3×10^{-8} M) (red line) with different concentrations of $(NH_4)_2[Ce(NO_3)_6]$ as oxidant in CF_3SO_3H (pH 1.0) solution based on the ruthenium catalytic units.

Kinetic studies.

To understand the water oxidation mechanisms in more details, the kinetic studies on catalysts **2** and **3** were carried out by monitoring the decay of Ce^{IV} at 360 nm with UV-Vis spectra (Figure 4a and 4c). Different amounts of catalysts were

injected into Ce^{IV} (1.5×10^{-3} M) aqueous solution and the data were collected after 2 seconds. The initial consumption rates of Ce^{IV} with catalyst **3** show a much steeper linear dependence on the catalyst concentrations with a first-order reaction constant of 36.31 s^{-1} (Figure 4d), which is higher than that of catalyst **2** with also a first-order reaction constant of 25.00 s^{-1} (Figure 4b). These results confirm again that catalyst **3** possesses much higher catalytic activity on water oxidation. In addition, the plots of log(rate) vs log([**2**]) and log([**3**]) have been calculated and shown in Figure S6. The slopes of the fitting linear are found to be 1.07 and 1.04, respectively. The results confirm again that the water oxidation of catalyst **2** and **3** are the first-order reaction. Overall, the obtained first-order kinetic constant indicates that no intermolecular reaction occurs during water oxidation process and the rate-determining step of O-O bond formation takes place most likely through intramolecular interaction. Nevertheless, the reaction mechanism of nucleophilic attack of water could not be totally excluded during this process.

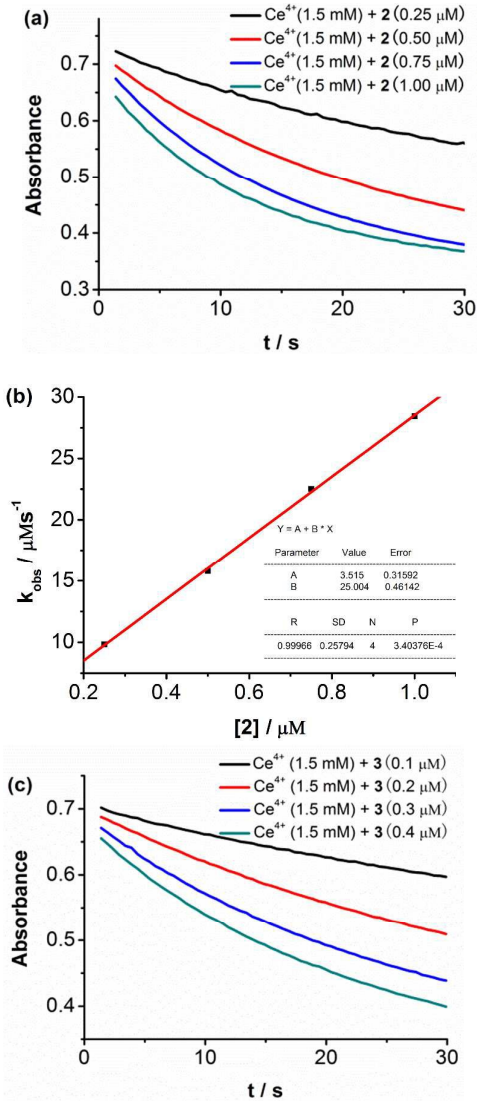

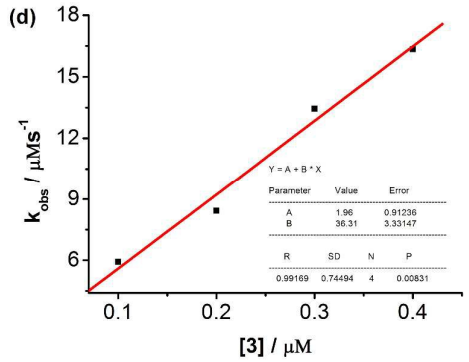

Figure 4. (a) Absorbance change at 360 nm according to catalyst **2** (0.25, 0.5, 0.75, 1.00 μM) addition into CF_3SO_3H (pH 1.0, 2.5 mL) solution containing Ce^{IV} (1.5×10^{-3} M). (b) Initial rates of Ce^{IV} consumption depend on the concentrations of catalyst **2**. (c) Absorbance change at 360 nm according to catalyst **3** (0.1, 0.2, 0.3, 0.4 μM) addition into CF_3SO_3H (pH 1.0, 2.5 mL) solution containing Ce^{IV} (1.5×10^{-3} M). (d) Initial rates of Ce^{IV} consumption depend on the concentrations of catalyst **3**.

Photocatalytic water oxidation.

The light driven water oxidation experiments were implemented in three component systems in phosphate buffer (pH 7.2) with complexes **1** (1×10^{-6} M), **2** (5×10^{-7} M) or **3** (3.3×10^{-7} M) as catalyst, $Ru(bpy)_2[4,4'\text{-}(EtOOC)_2\text{-}bpy)(PF_6)_2]$ (1×10^{-3} M) as photosensitizer, $Na_2S_2O_8$ (1×10^{-2} M) as sacrificial electron acceptor. The experiments were performed under 300 mW/cm^2 light intensity with 300 W Xe lamp passing through 400 nm filter at room temperature.

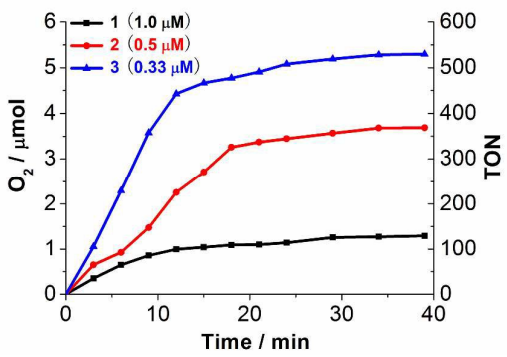

Figure 5. The light driven water oxidation measurements in three component systems in phosphate buffer (pH 7.2, 10 mL), with complexes **1** (1×10^{-6} M), **2** (5×10^{-7} M) or **3** (3.3×10^{-7} M) as catalysts, $Ru(bpy)_2[4,4'\text{-}(EtOOC)_2\text{-}bpy)(PF_6)_2]$ (1×10^{-3} M) as photosensitizer, $Na_2S_2O_8$ (1×10^{-2} M) as sacrificial electron acceptor; under 300 mW/cm^2 light intensity with 300 W Xe lamp passing through 400 nm filter at room temperature.

As shown in Figure 5, for the systems with catalysts **1**, **2** and **3**, the generated oxygen are collected respectively to be 1.29,

3.69 and 5.35 μmol, the relative TONs are calculated to be 129, 369 and 535. The obtained oxygen and TON from the system with catalyst **3** are substantially higher than those from the system with catalysts **1** and **2**. In addition, it is easy to find that the slope of oxygen generation curve for the system involving catalyst **3** is higher than that of catalysts **1** and **2** during the initial period of light illumination (12 minutes). These results also confirm that catalyst **3** is indeed superior to catalysts **1** and **2** on catalytic water oxidation, even in the photocatalytic process, keeping the same O-O bond formation mechanism of radical coupling within the trinuclear catalyst **3**. In addition, the better performance of catalyst **2** than catalyst **1** also indicates O-O bond formation through intramolecular reaction is better than intermolecular reaction.

Experimental

Synthetic procedures

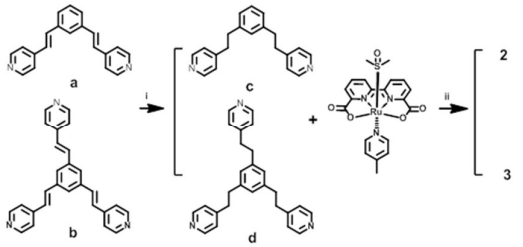

Scheme 1. Synthesis route of catalysts **2** and **3**. (i) H_2, Pd/C, EtOH, 2 days. (ii) CH_3OH, reflux, overnight.

General procedure for synthesis of compound a and b.

The synthesis of compounds **a** and **b** was carried out according to the reported literature.[24]

General procedure for synthesis of 1, 3-bis (4-pyridylethyl)-5-phenyl- phosphate c.

Compound **a** (1.8 g, 6.3 mmol), Pd/C (20 mg) were dissolved in EtOH (20 mL) in a 100 mL autoclave. The pressure of H_2 was controlled to be 10 normal atmospheres. The mixture was stirred under 100 °C for 24 hours and cooled to room temperature. Then Pd/C catalyst was filtered to recycle and the solvent was eliminated by rotary evaporator to give 1.7 g (94%) of compound **c** as a brown powder. ^{1}H NMR (400 MHz, $CDCl_3$) δ 8.29 (d, 4H), 7.19 (d, 2H), 7.13 (d, 2H), 6.75 (d, 4H), 2.84 (t, 8H). TOF-MS (ES+): m/z$^+$ 289.1687 $[M+H]^+$. Calcd: 289.1704.

General procedure for synthesis of 1, 3, 5-tri-(4-pyridyethyl)bezene d.

Compound **b** (1.9 g, 4.9 mmol), Pd/C (20 mg) were dissolved in EtOH (20 mL) in a 100 mL autoclave. The pressure of H_2 was controlled to be 10 normal atmospheres. The mixture was stirred under 100 °C for 24 hours and cooled to room temperature. Then Pd/C catalyst was filtered to recycle and the solvent was eliminated by rotary evaporator to give 1.85 g (96%) of compound **d** as a brown powder. ^{1}H NMR (400 MHz, $CDCl_3$) δ 8.37 –8.36 (m, 6H), 7.18 – 7.16 (m, 6H), 6.77 (s, 3H), 2.85 (t, 12H). TOF-MS (ES+): m/z$^+$ Found: 394.2278 $[M+H]^+$; Calcd: 394.2283.

General procedure for synthesis of complex 2.

A mixture of Ru(bda)(DMSO)(4-picoline) (300 mg, 0.6 mmol) and compound **c** (87 mg, 0.3 mmol) in dry CH_3OH (50 mL) was refluxed overnight under N_2 atmosphere. Then the solvent was removed under reduced pressure and the product was isolated by column chromatography on silica gel (CH_2Cl_2:CH_3OH = 10:1) to yield 80 mg (23%) of complex **2** as a dark red powder. ^{1}H NMR (400 MHz, d6-DMSO) δ 8.65 (d, J = 8.0 Hz, 4H), 7.88 (d, J = 6.8 Hz, 4H), 7.81 (t, J = 7.8 Hz, 4H), 7.53 (t, J = 6.0 Hz, 8H), 7.10 – 7.05 (m, 8H), 6.87 (d, J = 7.6, 1.3 Hz, 2H), 6.77 (s, 1H), 2.65 (d, J = 10.4 Hz, 8H), 2.19 (s, 6H). TOF-MS (ES+): m/z$^+$ Found: 1185.1406 $[M+Na]^+$; Calcd: 1185.1423. Elemental analysis, Calcd: For $C_{56}H_{46}N_8O_8Ru_2 \cdot CH_3OH \cdot 2H_2O$: C 55.78%, H 4.45%, N 8.86%; Found: C 55.60%, H 4.42%, N 9.11%.

General procedure for synthesis of complex 3.

A mixture of Ru(bda)(DMSO)(4-picoline) (300 mg, 0.6 mmol) and compound **d** (79 mg, 0.2 mmol) in dry CH_3OH (50 mL) was refluxed overnight under N_2 atmosphere. Then the solvent was removed under reduced pressure and the product was isolated by column chromatography on silica gel (CH_2Cl_2:CH_3OH = 5:1) to yield 40 mg (12%) of complex **3** as a dark red powder. ^{1}H NMR (400 MHz, d6-DMSO) δ 8.61 (d, J = 7.3 Hz, 6H), 7.79 (d, J = 7.5 Hz, 12H), 7.53 (s, 12H), 7.07 (s, 6H), 6.96 (s, 6H), 6.47 (s, 3H), 2.57 – 2.51 (m, 12H), 2.19 (s, 9H). TOF-MS (ES+): m/z$^+$ 1727.1924 $[M+Na]^+$; Calcd: 1727.1951. Elemental analysis, Calcd: For $C_{81}H_{66}N_{12}O_{12}Ru_3 \cdot 3H_2O$: C 55.42%, H 4.15%, N 9.39%; Found: C 55.28%, H 4.13%, N 9.56%.

Materials and methods

All reagent grade solvents were purchased from Aladdin chemical company, which were dried and distilled according to the standard methods. All other materials were commercially available. All reactions were carried out under N_2 atomosphere.

^{1}H NMR Spectra were collected at 298 K using a Bruker DRX-400 instrument. Electrospray ionization mass spectra and high resolution mass spectra were recorded on a Q-Tof Micromass spectrometer (Manchester, England). The cyclic voltammetry measurements were performed on a BAS-100W electrochemical potentiostat in a three-electrode system. The working electrode was a glassy carbon disk (diameter, 3 mm) polished with 3 and 1 mm diamond pastes and sonicated in ion-free water before use. The counter electrode was platinum wire. The reference electrode was Ag/AgCl. Oxygen evolution analyses were performed on a Techcomp GC 7890T instrument equipped with a 5 Å molecular sieve column and a thermal conductivity detector with argon as carrier gas and an oxygen sensor (OceanOptics NEOFOX-KIT-PATCH Non-Invasive oxygen monitoring kit and RE-FOS-4-KIT RedEye patch). The photo-

induce water oxidation experiments were performed under 300 mW/cm^2 light intensity with 300 W Xe lamp. The kinetic experiments were carried out on a HP 8450 spectrophotometer.

Conclusions

A highly efficient trinuclear catalyst **3** has been developed based on Ru-bda type of catalysts for water oxidation in homogeneous systems. Based on number of catalystic molecules, the TONs of catalyst **3** are found over two times higher than that of binuclear catalyst **2** in both chemically and photochemically driven catalytic water oxidation systems. Even based on the same number of active centers, the trinuclear catalyst **3** still displayed much higher efficiencies than the binuclear catalyst **2**. Kinetic studies demonstrate that the O-O bond formation catalyzed by the trinuclear complex **3** and the dinuclear complex **2** is through intramolecular radical coupling reaction. These results show that increasing the number of catalytic units within one catalyst molecule is beneficial to enhance the opportunity on formation of O-O bond. Further work on applying the highly efficient trinuclear catalyst **3** in dye-sensitized photoelectrochemical cell is undergoing.

Acknowledgements

This work was supported by the National Basic Research Program of China (973 program) (2014CB239402), the National Natural Science Foundation of China (20923006, 21120102036, 21106015, 91233201 and 21573033), the Fundamental Research Funds for the Central Universities (grant number DUT13RC(3)103, DUT15LK08), the Basic Research Project of Key Laboratory of Liaoning (LZ2015015), the Swedish Energy Agency and the K & A Wallenberg Foundation.

Notes and references

‡ Footnotes relating to the main text should appear here. These might include comments relevant to but not central to the matter under discussion, limited experimental and spectral data, and crystallographic data.
§
§§
etc.

1 V. K. Yachandra, K. Sauer, M. P. Klein, *Chem. Rev.,* 1996, **96**, 2927-2950.
2 C. W. Hoganson, G. T. Babcock, *Science,* 1997, **277**, 1953-1956.
3 W. Ruttinger, G. C. Dismukes, *Chem. Rev*., 1997, **97**, 1-24.
4 J. Limburg, J. S. Vrettos, H. Chen, J. C. Paula, R. H. Crabtree, G. W. Brudvig, *J. Am. Chem. Soc.,* 2001, **123**, 423-430.
5 M. Yagi, M. Kaneko, *Chem. Rev*., 2001, **101**, 21-35.
6 Y. Shimazaki, T. Nagano, H. Takesue, B. H. Ye, F. Tani, Y. Naruta, *Angew. Chem. Int. Ed.,* 2004, **43**, 98-100.
7 A. K. Poulsen, A. Rompel, C. J. McKenzie, *Angew. Chem. Int. Ed.,* 2005, **44,** 6916-6920.
8 R. Brimblecombe, G. C. Dismukes, G. F. Swiegers, L. Spiccia, *Dalton. Trans.,* 2009, **43**, 9374-9384.
9 S. W. Gersten, G. J. Samuels, T. J. Meyer, *J. Am. Chem. Soc.,* 1982, **104,** 4029-4032.
10 H. Yamada, W. F. Siems, T. Koike, J. K. Hurst, *J. Am. Chem. Soc.,* 2004, **126**, 9786-9795.
11 C. Sens, I. Romero, M. Rodríguez, A. Llobet, T. Parella, J. Benet-Buchholz, *J. Am. Chem. Soc.,* 2004, **126,** 7798-7799.
12 X. Yang, M-H. Baik, *J. Am. Chem. Soc.,* 2006, **128**, 7476-7485.
13 M. D. Karkas, T. Akermark, E. V. Johnston, S. R. Karim, T. M. Laine, B-L. Lee, T. Akermark, T. Privalov, B. Akermark, *Angew. Chem. Int. Ed.,* 2012, **51**, 11589-11593.
14 L. Duan, A. Fischer, Y. Xu, L. Sun, *J. Am. Chem. Soc.,* 2009, **131**, 10397-10399.
15 L. Duan, F. Bozoglian, S. Mandal, B. Stewart, T. Privalov, A. Llobet, L. Sun, *Nat. Chem.,* 2012, **4**, 418-523.
16 Y. Xu, A. Fischer, L. Duan, L. Tong, E. Gabrielsson, B. Akermark, L. Sun, *Angew. Chem. Int. Ed.,* 2010, **49**, 8934-8937.
17 Y. Jiang, F. Li, B. Zhang, X. Li, X. Wang, F. Huang, L. Sun, *Angew. Chem. Int. Ed.,* 2013, **52**, 3398-3401.
18 R. A. Binstead, C. W. Chronister, J. Ni, C. M. Hartshorn, T. J. Meyer, *J. Am. Chem. Soc.,* 2000, **122**, 8464-8473.
19 R. Zong, R. P. Thummel, *J. Am. Chem. Soc.,* 2005, **127**, 12802-12803.
20 N. D. McDaniel, F. J. Coughlin, L. L. Tinker, S. Bernhard, *J. Am. Chem. Soc.,* 2008, **130**, 210-217.
21 J. F. Hull, D. Balcells, J. D. Blakemore, C. D. Incarvito, O. G. Elsenstein, W. Brudvig, R. H. Crabtree, *J. Am. Chem. Soc.,* 2009, **131**, 8730-8731.
22 W. I. Dzik, S. E. Calvo, J. N. H. Reek, M. Lutz, M. A. Ciriano, C. Tejel, D. G. H. Hetterscheid, B. Bruin, *Organometallics,* 2011, **30,** 372-374.
23 M. D. Karkas, O. Verho, E. V. Johnston, B. Akermark, *Chem. Rev.,* 2014, **114**, 11863-12001.
24 A. J. Amoroso, A. M. W. Cargill Thompso, P. J. Maher, J. A. McCleverty, M. D. Ward, *Inorg. Chem.,* 1995, **34**, 4828-4835.
25 B. Li, F. Li, S. Bai, Z. Wang, L. Sun, Q. Yang, C. Li, *Energy Environ. Sci.*, 2012, **5**, 8229-8233.

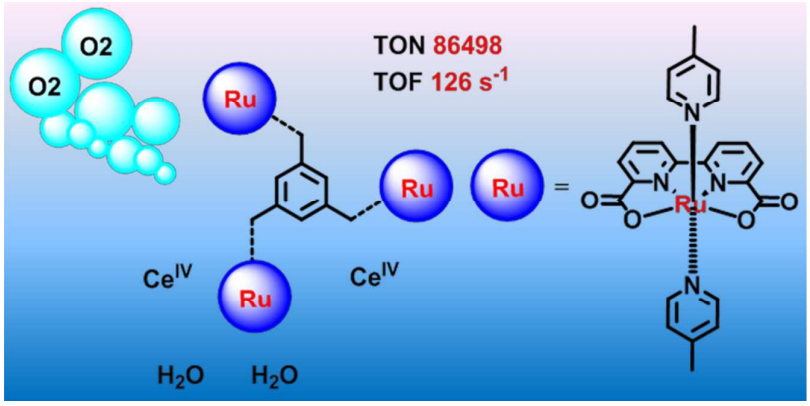

Trinuclear catalyst **3** was synthesized based on Ru(bda) (bda = 2, 2'-bipyridine-6,6'-dicarboxylic acid) type of catalysts for higher catalytic abilities in homogeneous water oxidation systems.